Hindawi
Advances in Civil Engineering
Volume 2019, Article ID 1643594, 12 pages
https://doi.org/10.1155/2019/1643594

Research Article

Estimating the Effects of Tunnelling on Preexisting Jointed Pipelines

Shao Yu,[1,2,3] Zhibo Duan,[1] Ying Liu,[4] Min Ma,[5] and Shaokun Ma[6]

[1]*Ph.D., College of Civil Engineering and Architecture, GuangXi University, Nanning 530004, China*
[2]*Ph.D. Research Assistant, Guangxi Xinfazhan Communications Group Co., Ltd, Nanning 530029, China*
[3]*Ph.D. Research Assistant, Guangxi Road and Bridge Engineering Group Co., Ltd., Nanning 530011, Guangxi, China*
[4]*Lecturer, College of Civil Engineering and Architecture, GuangXi University, Nanning 530004, China*
[5]*Master Degree Candidate, College of Civil Engineering and Architecture, GuangXi University, Nanning 530004, China*
[6]*Professor, College of Civil Engineering and Architecture, GuangXi University, Nanning 530004, China*

Correspondence should be addressed to Shaokun Ma; mashaokun@sina.com

Received 30 March 2019; Revised 5 June 2019; Accepted 11 June 2019; Published 25 June 2019

Academic Editor: Tayfun Dede

Tunnel excavation inevitably results in ground movements and changes in soil stress, leading to additional stress on and settlement of nearby buried pipelines. This article focuses on the response of jointed pipelines to twin tunnelling. The relationship between the relative pipe-soil displacement and the relative pipe-soil stiffness was first determined. Based on this analysis, a series of numerical parametric studies encompassing 7776 conditions were performed to investigate the responses of a jointed pipeline to twin tunnelling. The results are used to estimate a regression equation for the relationship between the relative pipe-soil stiffness and the normalized maximum joint rotation angle. This equation can be used for the direct calculation of the maximum joint rotation angle that will result from single or twin tunnelling and for the assessment of the tunnelling-induced risk to jointed pipelines. The applicability and reliability of the regression equation are validated by comparing the calculated values with the results of earlier centrifuge tests.

1. Introduction

Underground space is becoming increasingly utilized in urban spaces, and this has resulted in growing research interest in the effects of tunnel construction on pre-existing structures, especially pre-existing underground pipelines. Tunnel excavation often causes less additional strain in pipelines with joints (where the stiffness at the joints is less than the stiffness of the pipelines, collectively referred to herein as jointed pipelines) than in continuous pipelines (where the stiffness at the joints is greater than the stiffness of the pipelines) because the joints give them added flexibility [1]. However, such pipelines often become damaged or broken because joint rotation can cause the pipeline to leak or even explode. Therefore, when designing jointed pipelines, engineers often use the allowable rotation of the joints as the main design criterion, while the allowable additional strains in the pipelines are considered to be auxiliary design constraints.

Valuable geotechnical research has been conducted on the response of jointed pipelines to tunnelling-induced ground movement using both analytical methods and numerical simulation. The Winkler model has been used to evaluate the impact of tunnel excavation on jointed pipelines [2], and an analytical method has been used to explore the specific impacts of different pipe-to-soil stiffness ratios (herein referred to as relative pipe-soil stiffness), different relative pipe-joint stiffnesses, and different joint locations relative to the tunnel centreline [1]. Recently, numerical simulation has been employed to analyze the effect of single-tunnel excavation on jointed pipelines and has provided a formula for predicting the joint rotation that will be caused by single-tunnel excavation under a variety of operating conditions [3]. Finite element analysis and large-scale

laboratory modelling have been adopted to assess the responses of pig iron jointed pipelines and ductile cast iron jointed pipelines to single-tunnel excavation and have found pig iron jointed pipeline to be the type that is more affected and more easily damaged by tunnel excavation [4].

Indoor shrinkage modelling has been employed to study the development of subsidence, underground pipeline deformation, and surface settlement in dry sand [5]. Meanwhile, numerical modelling has been used to construct a dimensionless plot relating relative pipe-soil stiffness with the ratio of maximum pipe curvature to maximum ground curvature; this plot can be used to directly estimate the maximum curvatures of pipelines subjected to normal fault movement [6]. In terms of experimental work, centrifuge tests have been conducted to investigate the three-dimensional response of the ground and a pipeline to tunnelling, considering different pipeline orientations with respect to the tunnelling direction [7]. Further centrifuge tests have been used to investigate the influence of tunnel excavation on jointed pipelines specifically, taking into account different amounts of volume loss and different joint locations relative to the tunnel centreline [8]. Centrifuge tests have also been employed to explore the effects of fault formation on pipelines and joints and have shown that the maximum joint rotation angle caused by a normal fault is greater where the associated plastic shear zone passes through a pipeline joint than when it passes between two joints [9]. BOTDR (brillouin optical time-domain reflectometry) fibre optic sensors have been used to monitor the strain induced in socket-injected jointed pipelines by tunnelling via the top tube method [10].

In this study, finite element analysis was used to study the impact of twin-tunnel excavation on pre-existing pipelines, and a series of numerical parametric studies encompassing 7776 conditions were carried out to explore the phenomenon in more depth. On the basis of the results obtained, a regression equation is presented that predicts the maximum joint rotation angle associated with single and twin-tunnel excavation.

2. Settlement Caused by Twin-Tunnel Excavation

A modified Gaussian distribution curve with the following form has been proposed to describe the soil settlement caused by tunnel excavation [11]:

$$S_v(x) = \frac{nS_{max}}{(n-1) + \exp[\alpha(x^2/i^2)]}, \quad (1)$$

$$n = \exp(\alpha)\frac{2\alpha - 1}{2\alpha + 1} + 1, \quad (2)$$

where $S_v(x)$ is the greenfield settlement, S_{max} is the maximum vertical displacement of the soil above the tunnel centreline, i is the distance between the tunnel centreline and the inflexion point of the ground settlement trough, and n and α are shape parameters of the settlement trough in the soil. When $\alpha = 0.5$ and $n = 1$, formula (1) degenerates to the form of a Gaussian distribution curve.

The abovementioned modified Gaussian curve achieves a better fit to ground settlement values obtained from field measurement and centrifugal model tests than other empirical formulas describing the surface settlement troughs caused by tunnel excavation [12]. Furthermore, an even better fit may be achieved when a series of Gaussian distribution curves are superimposed [13]. Specifically, analysis of field data indicates that the ground settlement curve caused by twin-tunnel excavation can be fitted well by the superimposition of two sets of Gaussian distribution curves [14]. Therefore, this paper selects the modified Gaussian distribution curve as the most appropriate way to describe the ground settlement trough caused by twin-tunnel excavation.

3. Pipe-Soil Interaction

The range over which the pipe and soil interact is divided into the following five regions: the downwards compression zone, the pulldown zone, the stretching zone, the zone not influenced by the pipeline, and the pipeline-soil detachment zone [10, 15]. In practical applications, the hyperbolic model is often used to describe the vertical (i.e., the solid line in Figure 1) and axial (i.e., the solid line in Figure 2) interactions between the pipe and the soil. For ease of use, these are simplified to a combination of an elastic and ideal elastoplastic model (the solid lines in Figures 1 and 2).

In Figure 1, q_u and q_d are the maximum resistances of the soil when the relative displacement of the pipe versus the soil (herein referred to as the relative pipe-soil displacement) is upward and downward, respectively. The magnitude of this resistance is closely related to the relative displacement and can be expressed as follows [16–19]:

$$q_u = N_v \gamma H D,$$
$$q_d = \gamma H N_q D + \frac{1}{2}\gamma D^2 N_\gamma, \quad (3)$$

where N_v is the dimensionless soil resistance coefficient, N_q and N_γ are Vesic's bearing capacity factors for vertical strip footings, γ is the bulk unit weight of the soil, H is the distance from the ground to the centre of the pipeline, and D is the outer diameter of the pipeline.

Figure 1 shows the associated thresholds of relative pipe-soil movement, δ_{ru} and δ_{rd}. That is, when the relative pipe-soil displacement upward and downward exceeds δ_{ru} and δ_{rd}, the resistance of the soil will reach q_u and q_d, respectively. When the soil compaction is in the loose to dense sand range, the values of δ_{ru} and δ_{rd} are $0.005–0.015H$ and $0.1–0.15D$, respectively [18]. In Figure 2, q_a is the maximum resistance of the soil when the relative axial pipe-soil displacement reaches δ_{ra}. When the pipeline is buried in sand, the value of δ_{ra} is 2.5–5.0 mm [18]. q_a can be calculated with the following formula [18]:

$$q_a = \frac{1}{2}\pi D\gamma H(1 + K_0)\tan\delta, \quad (4)$$

where K_0 is the static pressure coefficient of the soil and δ is the friction angle of the pipe-soil contact surface.

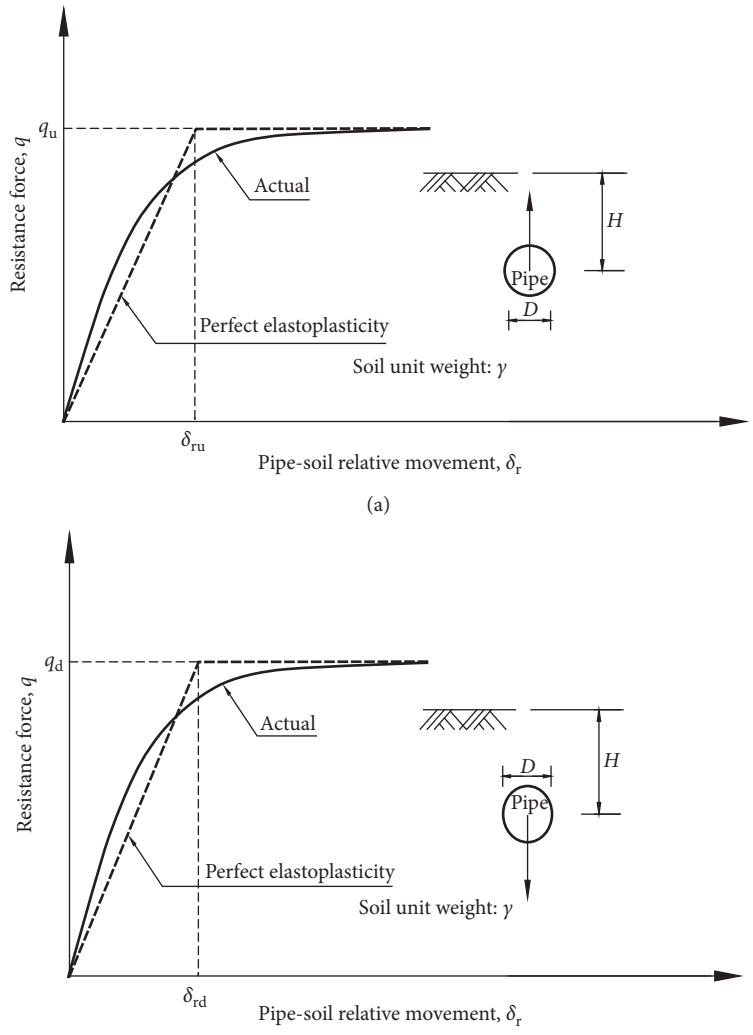

Figure 1: Force-displacement response in pipe-soil interaction. (a) Upward relative movement of the pipe versus the soil. (b) Downward relative movement of the pipe versus the soil.

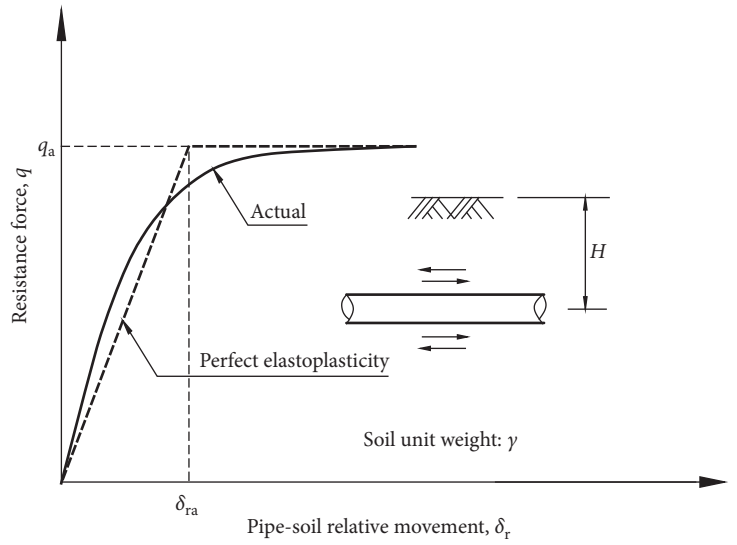

Figure 2: Force-axial relative displacement response in pipe-soil interaction.

4. Calculation Method and Validation

4.1. Calculation Method. Real-world monitoring projects often use the hoop method to measure pipeline deformation, but this can be difficult to implement, so this study instead employs the values that would be derived by surface subsidence monitoring. Figure 3 shows the vertical and axial pipe-soil interactions that will occur when the maximum greenfield ground settlement caused by twin-tunnel excavation is directly below a joint or a pipe section. The interactive relationships are embedded in the ABAQUS software PSI (pipeline soil interaction), and different interactions are used for the calculations according to the current relative displacement of the pipe and soil. Internal forces and deformations generated by external loads on the pipeline are described using beam elements. The DISP subroutine is programmed according to equation (1). The greenfield ground settlement caused by tunnelling is applied to the surface as distributed displacement, as shown in Figure 3.

When pipe sections use connectors such as rubber gasket push-in joints, mechanical bolt-gland joints, and mechanical rubber gland couplings, the pipeline can be regarded as a jointed pipeline. Due to the significantly weakened bending moment transmission in this kind of flexible-jointed pipeline, the mechanical behaviour of the joints is best simplified as that of a hinge [2]. It should be noted that experimentation has indicated that the behaviour of a nodal pipeline is more complex than encompassed by the hinge model [20, 21]. For example, a hinge can limit the axial translation and translation axial stress of the jointed pipeline, which may not accord with the actual situation. However, the main purpose of this research is to study joint rotation induced by twin tunnelling rather than the axial behaviour of the pipeline, so hinges are used to simulate pipeline joints.

4.2. Model Validation. Two types of centrifuge test were performed by Vorster et al. to study the effect of tunnel excavation on jointed pipelines [10]. In one set of tests, the tunnel centreline was located directly below a joint (J1), and in the other set, the tunnel centreline was located just below the centre of a pipe segment (J2). The tests were carried out at $75g$, where g is gravitation acceleration. In each test, a jointed pipeline with a diameter of 1.19 m and thickness of 0.09 m (in prototype) was buried so that the pipe centre was at a depth (H) of 4.165 m, which equates to $C_p/D_p = 2.0$ (the ratio of the soil thickness to the pipe diameter). The pipe segments were made of aluminium, and the joints were made of PVC. A 1.5–2.0 mm space was left between each pair of consecutive pipe segments to allow for rotation. Compared with those of the individual pipe segments, the moment capacity and axial rigidity of the PVC joints can be ignored. The model pipeline consists of nine aluminium pipe segments (each 5.34 m long in prototype) and eight PVC joints, and the length of the pipeline is 52.4 m (prototype) in total. Figure 4 illustrates the deformed pipe segments schematically. An LVDT (linear variable differential transformer, a displacement sensor) extension rod was installed along each pipe segment to measure vertical displacement. The measured differential pipe settlement and the distance between the two measurement points could then be used to obtain the slope of each pipe segment. These were summed to obtain the joint rotation angle, as follows:

$$\theta = \theta_1 + \theta_2,$$

$$\theta_1 = \arctan\left(\frac{S_{p1} - S_{p2}}{x_1 - x_2}\right), \tag{5}$$

$$\theta_2 = \arctan\left(\frac{S_{p3} - S_{p4}}{x_3 - x_4}\right),$$

where $S_{p1} - S_{p2}$ and $S_{p3} - S_{p4}$ are the differential pipe settlements and $x_1 - x_2$ and $x_3 - x_4$ are the distances between the two measured points.

Figure 5 shows a comparison between the maximum rotation angle of the pipeline joint derived by calculation and by measurement in the centrifugal test. The relative upward and downward displacements of the pipe and soil were taken to be $\xi_{ru} = 0.01H$ and $\xi_{rd} = 0.01D_p$, respectively. Regardless of whether the tunnel centreline was located below a joint or below the centre of a pipe segment, the measured joint rotation caused by tunnel excavation increases with an increase in tunnel volume loss. Thus, the rotation angle of jointed pipelines is sensitive to tunnel volume loss. The calculated values for maximum joint rotation are very consistent with the measured values under the four conditions.

5. Influence of the Relative Positions of Maximum Soil Displacement and of Joints

The influence of the relative positions of a joint and of maximum ground settlement on a jointed pipeline was next explored by considering two pipe segment lengths ($L_s = 4.8$ m and 7.2 m) and two pipe diameters ($D_p = 0.14$ m and 0.51 m). These variables are paired to construct four jointed pipelines, each 240 m long, which are buried in loose sand. The distance from the ground surface to the top of the pipeline is 1.2 m. The angle of internal friction and the bulk unit weight of the sand are 30° and 16 kN/m^3, respectively. The relative pipe-soil displacements upward and downward are taken to be $\xi_{ru} = 0.01H$ and $\xi_{rd} = 0.01D_p$, respectively.

Figure 6 shows the influence of the relative positions of a joint and of maximum ground settlement on a jointed pipeline. In the figure, d is the distance between the locus of maximum displacement of the greenfield and the midpoint of the pipe segment. From Figure 6(a), it can be seen that the maximum joint rotation angle is smallest when the maximum ground settlement is located below the centre of a pipe segment. As the relative horizontal distance to a joint decreases, the maximum joint rotation angle gradually increases. When maximum ground settlement is below a joint, the maximum joint rotation angle is at its largest. Thus, the minimum and maximum joint rotation angles appear when the maximum ground settlement is located below the centre of a pipe segment and below a joint, respectively. The

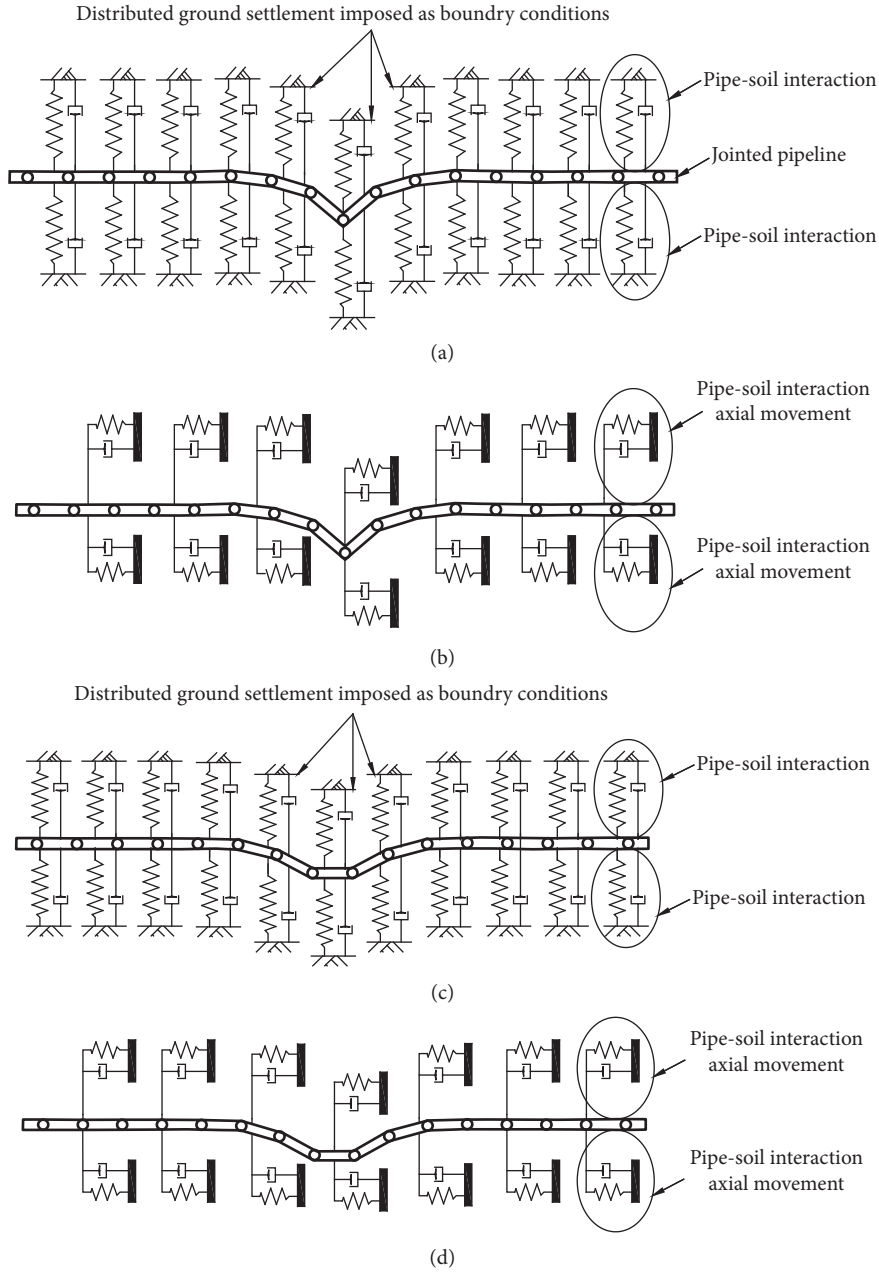

Figure 3: Schematic diagrams of pipe-soil interaction. (a) Vertical pipe-soil interaction (when the maximum ground settlement is located beneath a joint). (b) Axial pipe-soil interaction (when the maximum ground settlement is located beneath a joint). (c) Vertical pipe-soil interaction (when the maximum ground settlement is located beneath the centre of pipe segment). (d) Axial pipe-soil interaction (when the maximum ground settlement is located beneath the centre of pipe segment).

maximum and minimum joint rotation angles are the upper and lower limits, respectively, for working conditions in case of twin-tunnel excavation. It can be seen from Figure 6(a) that the diameter of the pipeline has a greater influence on the maximum joint rotation angle than does its length. The effect of the relative stiffness of the pipe versus that of the soil on the maximum joint rotation angle is investigated in Section 7.

Figure 6(b) shows the influence of the relative locations of a joint and of maximum ground settlement on the maximum bending strain in the jointed pipeline. This exhibits the opposite trend to the effect on joint rotation. The maximum bending strain in the jointed pipeline is at its highest value when the locus of maximum ground settlement is beneath the centre of a pipe segment. As the relative horizontal distance to a joint decreases, the maximum bending strain in the pipeline gradually increases, and it reaches a minimum when the maximum ground settlement is beneath the joint. This is consistent with Figure 6(c), which shows the influence of the relative positions of a joint and of maximum ground settlement on the maximum displacement of the jointed pipeline [1]. The maximum displacement

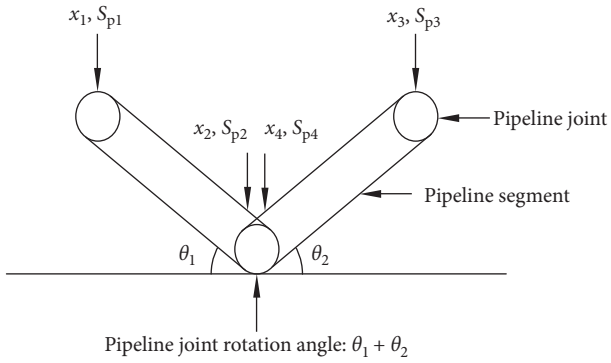

Figure 4: Definition of the joint rotation angle.

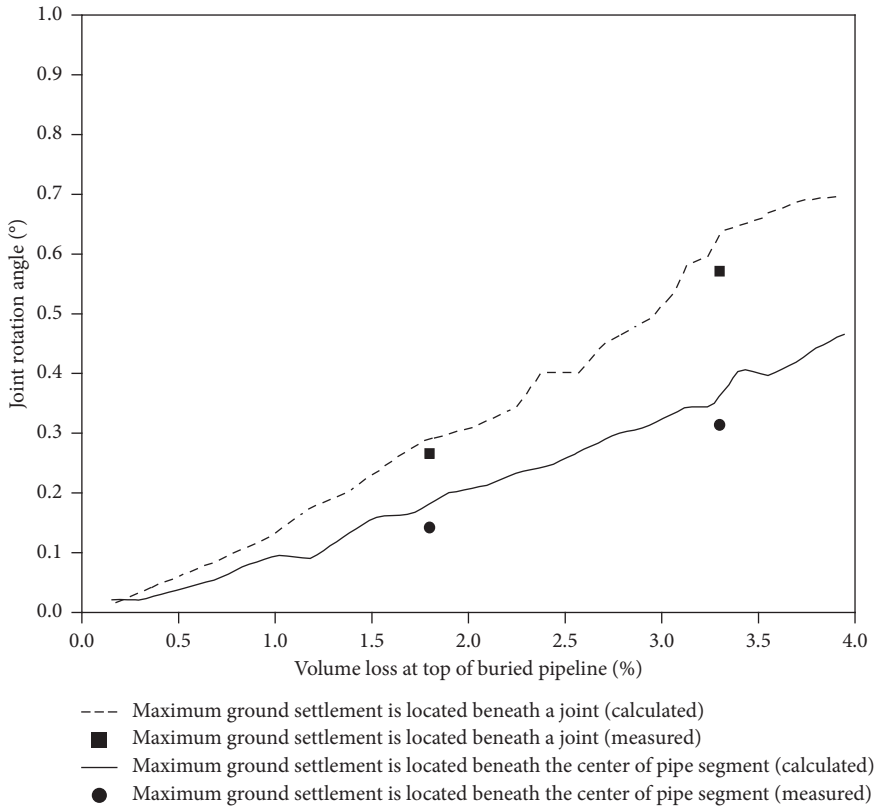

Figure 5: Comparison of measured and computed joint rotation.

of the pipeline is lowest when the maximum ground settlement is located directly below the centre of a pipe segment and gradually increases as the relative horizontal distance to a joint decreases. However, the relative location of a joint and of maximum settlement has less influence on the maximum displacement of the jointed pipeline than it does on the other parameters investigated here; the difference between the maximum and minimum vertical displacement is only about 7.5% of the minimum displacement value.

The above analysis indicates that the influence of twin-tunnel excavation on a jointed pipeline is largest when the maximum ground settlement is located below a joint and is at a minimum when the maximum settlement is below the midpoint of a pipe segment. Although the maximum bending strain that is caused to the jointed pipeline by twin-tunnel excavation is smaller under the former condition than under the latter, the maximum joint rotation angle is larger. The current reference standard for jointed pipeline design is mainly based on the joint rotation angle, with the bending strain on pipe segments considered as a supplementary factor. The effect of twin-tunnel excavation will thus be considered to be greatest when the maximum ground settlement is located beneath a joint.

6. Method of Parametric Analysis

The cases where the maximum ground movement induced by twin tunnelling is located directly below the centre of a

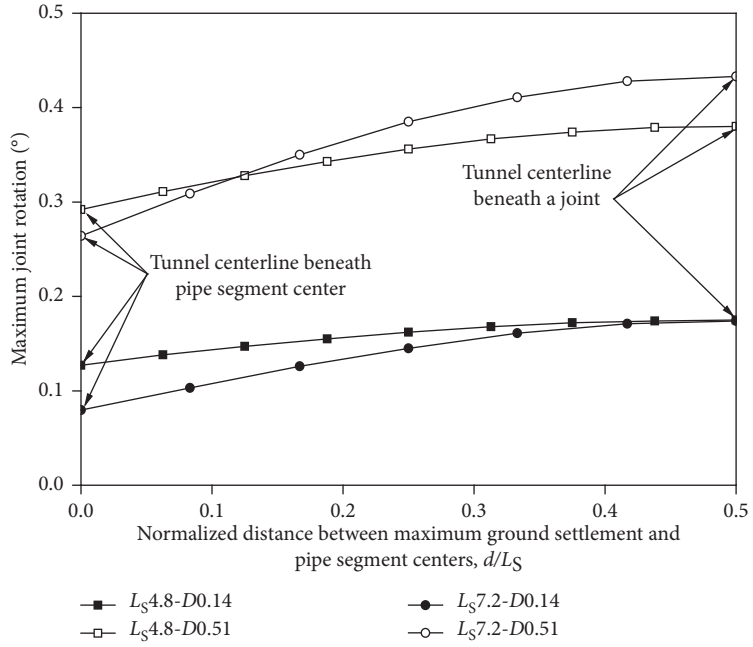

(a)

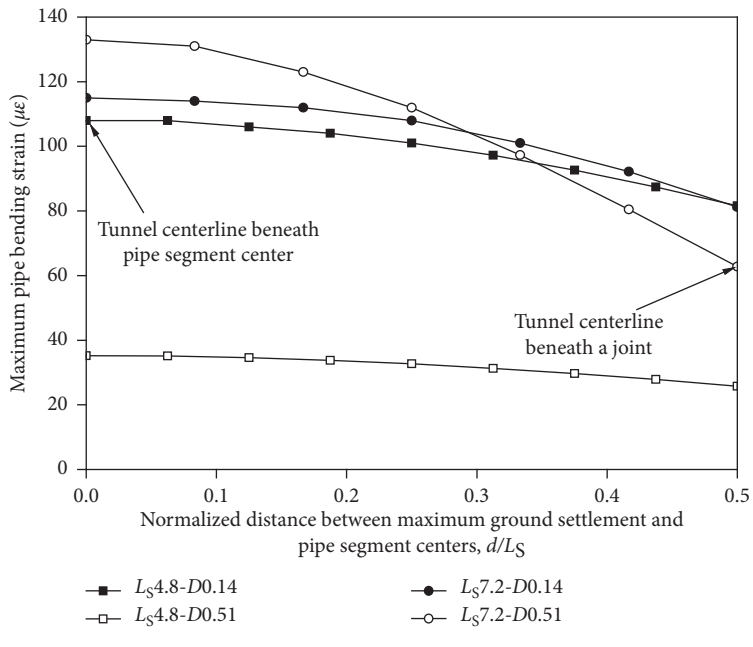

(b)

Figure 6: Continued.

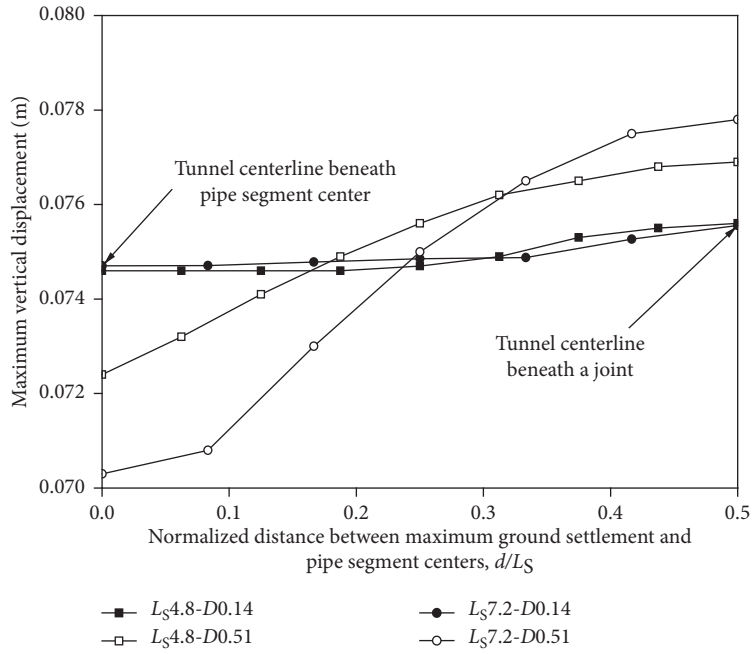

(c)

Figure 6: Influence of the distance between a joint and the locus of maximum ground settlement on a jointed pipeline. (a) Influence of the distance between a joint and the locus of maximum ground settlement on maximum joint rotation. (b) Influence of the distance between a joint and the locus of maximum ground settlement on maximum pipe bending strain. (c) Influence of the distance between a joint and the locus of maximum ground settlement on maximum vertical displacement.

pipe segment and below a joint were next analyzed for a variety of working conditions. The above analysis indicates that it is only necessary to set reasonable parameters for the ground settlement curve caused by tunnel excavation (S_{max}, i, and α): the size parameters of the pipeline (diameter D and wall thickness T), the material parameters of the pipeline (elastic modulus E and Poisson's ratio ν), the pipe length (L_s), and the soil thickness C above the pipeline and the soil parameters (γ and φ). The upward and downward relative displacements of the pipe versus the soil are taken as $\xi_{ru} = 0.01H$ and $\xi_{rd} = 0.01D_p$, respectively. To determine reasonable values for the influence of twin-tunnel excavation on the maximum joint rotation, this section adopts the ranges in the above parameters that are commonly used in practical engineering contexts. On that basis, a series of numerical parametric studies were performed encompassing 7776 conditions. In 3888 of them, the maximum ground settlement caused by twin-tunnel excavation was located below a pipe segment centre, and in the other 3888, it was below a joint. The results of this analysis could then be used to obtain the maximum joint rotation angle caused in pre-existing pipelines by twin-tunnel excavation under a wide range of working conditions.

S_{max}, I, and α took values in the range of 0.025–0.3 m, 2–12 m, and 0.1–1.8 m, respectively, covering the conditions common for surface subsidence caused by the twin-tunnel excavation of urban subways. Tables 1 and 2 list the pipeline sizes and material parameters used in the calculations, respectively. The values of these parameters are those commonly in use for municipal engineering. Three values were used for overburden thickness (C), 1.2 m, 2.4 m, and 4.0 m, and four pipe lengths (L_s) were adopted, 2.4 m, 4.8 m, 7.2 m, and 9.6 m. The parameters relating to the three selected soil densities are listed in Table 3.

Table 1: Summary of the pipeline dimension.

Pipeline dimension	Pipe 1	Pipe 2	Pipe 3	Pipe 4	Pipe 5
Diameter, D (m)	0.14	0.51	0.81	1.02	1.31
Wall thickness, T (mm)	6	10	13	26	38

Table 2: Summary of the material properties of the pipeline.

Pipeline material properties	Elastic modulus (GPa)	Poisson ratio
Concrete	35	0.3
Cast iron	84	0.3
Steel	210	0.3

7. Dimensional Analysis of the Influence of Tunnel Excavation on Pipelines

An analytic method was used previously to explore the effect of single-tunnel excavation on pre-existing pipelines [1] and arrived through dimensional analysis of calculation results at a normalized processing formula for the joint rotation angle of $(\theta \cdot i/S_{max})$, where S_{max} and i are the parameters of the vertical ground settlement. In this paper, a modified Gaussian curve is used to describe the vertical ground settlement induced by twin-tunnel excavation. The

Table 3: Summary of the soil properties.

Soil properties	Loose sand	Medium sand	Dense sand
Friction angle, φ (°)	30.0	35.0	40
Bulk unit weight, γ (kN/m^3)	16.0	17.5	19.0

normalized processing formula of the joint rotation angle considers the influence of the parameters S_{max}, i, α, and n on the calculation result, and the expression is $\theta \cdot i\,(n/2\theta)^{0.5}/S_{max}$. Another formula is proposed to express the ratio of the stiffness of the pipe to that of the soil (the relative pipe-soil stiffness, R) during twin-tunnel excavation:

$$R = \left[\frac{E_p I_p}{K_u^{0.9} K_d^{0.1}\left((n/2\alpha)^{0.5} i\right)^4}\right] \cdot \left[\frac{i}{L_s}\right]^{0.5}, \tag{6}$$

$$K_u = \frac{q_u}{\delta_{ru}}, \qquad K_d = \frac{q_d}{\delta_{rd}}, \tag{7}$$

where E_pI_p is the flexural stiffness of the pipeline and K_u and K_d are the equivalent moduli when the relative pipe-soil displacement is upward and downward, respectively.

Figure 7 shows dimensionless plots for the relative pipe-soil stiffness versus the normalized maximum joint rotation angle for the 7776 conditions studied. The figure indicates that the expressions for the relative pipe-soil stiffness and the relative rotation angle are reasonable and that they can be applied to the normalization of the calculation results. Figure 7(a) shows that when the maximum ground settlement is located below a joint and the relative pipe-soil stiffness is below 0.264, the joint rotation angle gradually increases with an increase in relative pipe-soil stiffness. When the relative pipe-soil stiffness is more than 0.264, the joint rotation angle decreases with an increase in the relative pipe-soil stiffness. Meanwhile, Figure 7(b) shows that when the maximum ground settlement is located below the centre of a pipe segment, the joint rotation angle increases with an increase in the relative pipe-soil stiffness up to a relative stiffness of 0.052 and then decreases as relative stiffness increases beyond that value. In other words, when the maximum ground settlement is located beneath a joint, the pipeline can be regarded as a flexible-jointed pipeline when the relative pipe-soil stiffness is less than 0.264 and as a stiff-jointed pipeline at higher relative pipe-soil stiffness values. When the maximum ground settlement is located below the centre of a pipe segment, this threshold value between pipeline behaviours lies at a relative pipe-soil stiffness of 0.052.

A regression analysis was conducted on the curves in Figures 7(a) and 7(b) to arrive at the following equations:

When the maximum ground settlement is located below a joint,

$$y = \frac{15.7}{0.85\,(\ln R + R^{0.5} + 0.9)^2 + 17.0}. \tag{8}$$

When the maximum ground settlement is located below the centre of a pipe segment,

$$y = \frac{10.0}{1.2\,(\ln R^{0.84} + R + 2.5)^2 + 19.0}. \tag{9}$$

In these equations, R is the relative pipe-soil stiffness expressed as $[E_pI_p/K_u^{0.9}K_d^{0.1}\,((n/2\alpha)^{0.5}i)^4] \cdot [i/L_s]^{0.5}$ and y is the normalized joint rotation angle expressed as $\theta \cdot i\,(n/2\alpha)^{0.5}/S_{max}$.

No field measured data have yet been published on the impact of twin-tunnel excavation on existing jointed pipelines, and the subject has seen little study. However, centrifuge tests have been conducted to explore the effect of single-tunnel excavation with different volume loss values on pre-existing jointed pipelines [11]. These tests considered a tunnel centreline either below a joint or below the centre of a pipe segment. Figure 8 provides a comparison of the computational results from this study and the results of the centrifuge tests in Vorster et al. [11].

It is proposed that the calculation formula can be used not only to calculate the maximum joint rotation angle caused by single-tunnel excavation but also that caused by twin-tunnel excavation. This can be illustrated by performing calculations according to the following scenario. Consider a concrete pipe with a diameter of 0.75 m, a wall thickness of 14 mm, an elastic modulus of 35 GPa, and a flexural stiffness of 76.74 GPa that is buried so that the distance between the tunnel centreline and the surface is 1.8 m. The parameters of the ground settlement caused by twin-tunnel excavation are $S_{max} = 0.075$ m, $\alpha = 0.35$, and $i = 3.5$ m; the peak friction angle of the soil is 37.5°, and the bulk unit weight of the soil is 19 kN/m^3. $\delta_{ru} = 0.01H = 0.027$ m, $\delta_{rd} = 0.1D = 0.09375$ m, and q_u and q_d are 52.47 kN/m and 154.97 kN/m, respectively. Equation (7) gives values for K_u and K_d of 1.94 MPa and 16.53 MPa, respectively. The relative pipe-soil stiffness is then $[E_pI_p/K_u^{0.9}K_d^{0.1}\,((n/2\alpha)^{0.5}i)^4] \cdot [i/L_s]^{0.5} = 0.1971$. When the maximum ground settlement caused by twin-tunnel excavation is located beneath a joint, formula (8) gives $\theta \cdot i\,(n/2\alpha)^{0.5}/S_{max} = 0.9199$, and the maximum joint rotation angle caused by the twin-tunnel excavation is $\theta = 0.01938 = 1.111°$. When the maximum ground settlement is located below the centre of a pipe segment, formula (9) gives $\theta \cdot i\,(n/2\alpha)^{0.5}/S_{max} = 0.4732$, and the maximum joint rotation angle caused by twin-tunnel excavation is $\theta = 0.009966 = 0.571°$. Both values exceed the allowable corner value (0.275°) [22].

8. Evaluation of the Responses of Adjacent Pipelines to Tunnel Excavation

When the maximum joint rotation of a cast iron pipeline lies within the serviceability range 0.54–0.92°, the pipeline is destroyed [22]. The maximum allowable joint rotation angle of the pipeline is affected by many factors such as the degree of corrosion of the joint before tunnel excavation, the connection mode of the joint, and the loading of the joint. If the allowable joint rotation angle used for pipeline design is

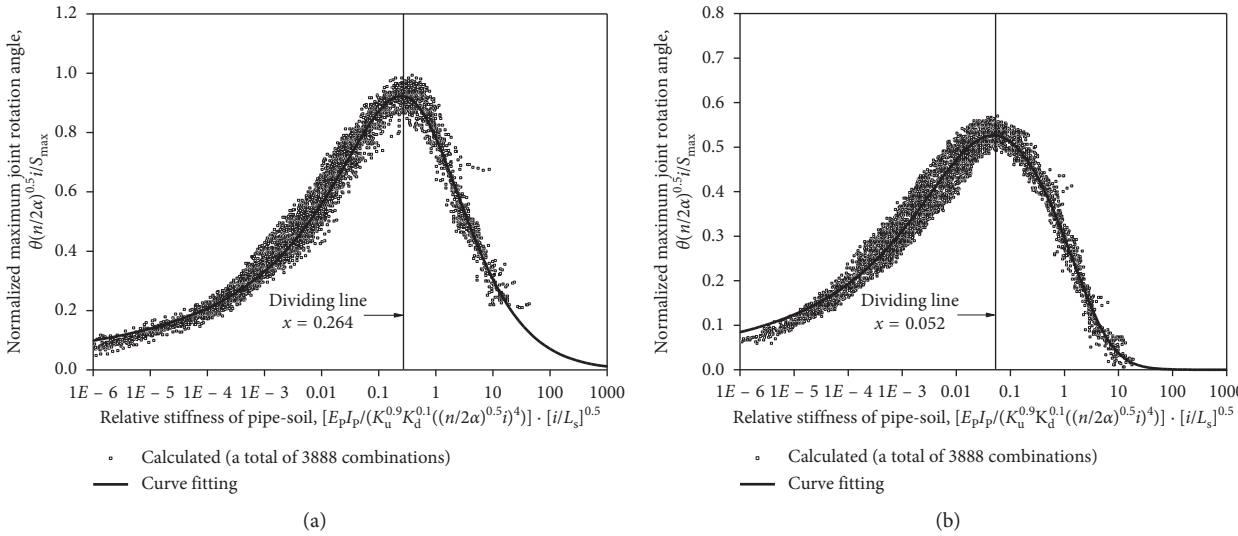

Figure 7: Dimensionless plots of pipe-soil relative stiffness versus normalized maximum joint rotation angle. (a) The maximum ground settlement is located beneath a joint. (b) The maximum ground settlement is located beneath the centre of pipe segment.

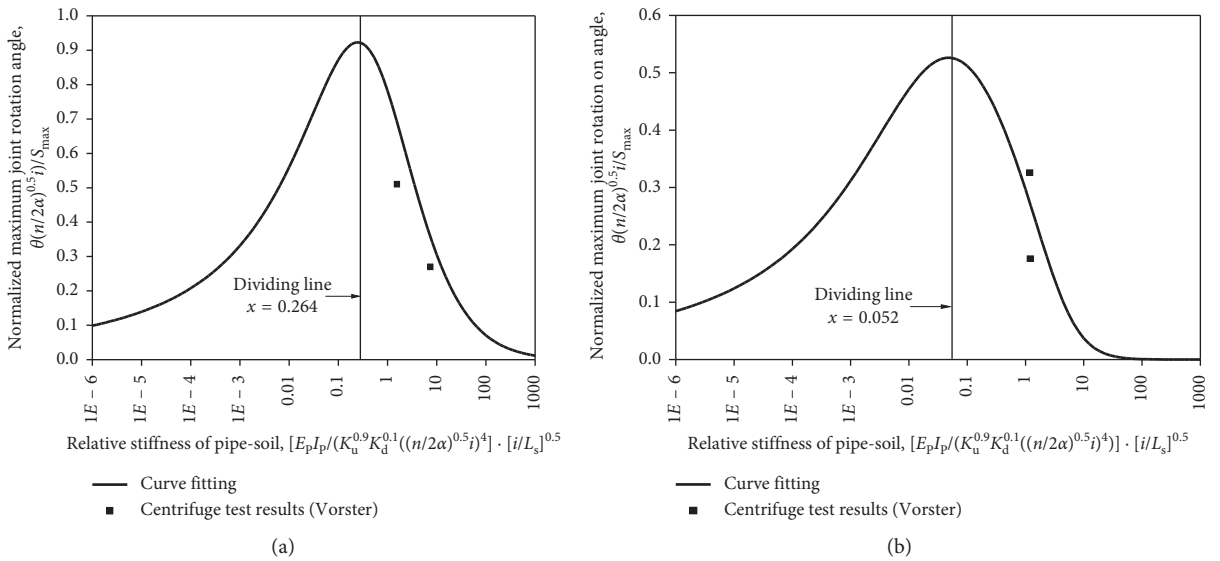

Figure 8: Comparison of computational results and centrifuge test results. (a) The maximum ground settlement is located beneath a joint. (b) The maximum ground settlement is located beneath the centre of a pipe segment.

$\theta_{pallowable} = 0.73^{\circ}$, equations (8) and (9) can be written as follows:

$$\frac{S_{max}}{(n/2\alpha)^{0.5}i} = \frac{0.85\left(\ln R + R^{0.5} + 0.9\right)^2 + 17.0}{15.7}\theta_{pallowable},$$

$$\frac{S_{max}}{(n/2\alpha)^{0.5}i} = \frac{1.2\left(\ln R^{0.84} + R + 2.5\right)^2 + 19.0}{10.0}\theta_{pallowable}. \quad (10)$$

Figure 9 illustrates the relationship between boundary curves based on jointed pipeline safety criteria and the effects of tunnelling where maximum settlement occurs at different locations. The scenario outlined in Section 7 is used as an example and is indicated with a solid square. This calculated value lies between the two boundary curves. Thus, for the working conditions adopted in the example, when the maximum ground settlement is located beneath a joint, the jointed pipeline is in an unsafe state and the pipeline will become unserviceable due to a large joint rotation angle. However, when the maximum ground settlement is located below a pipe segment centre, the jointed pipeline is in a safe state. Figure 9 also shows the results of two sets of centrifugal tests conducted by Vorster et al. [10]. When the volume loss is 1% or 2%, the jointed pipeline is in a normal working condition both when the maximum ground settlement is beneath a joint and when it is beneath the centre of a pipe segment. With an increase in volume loss, the predicted

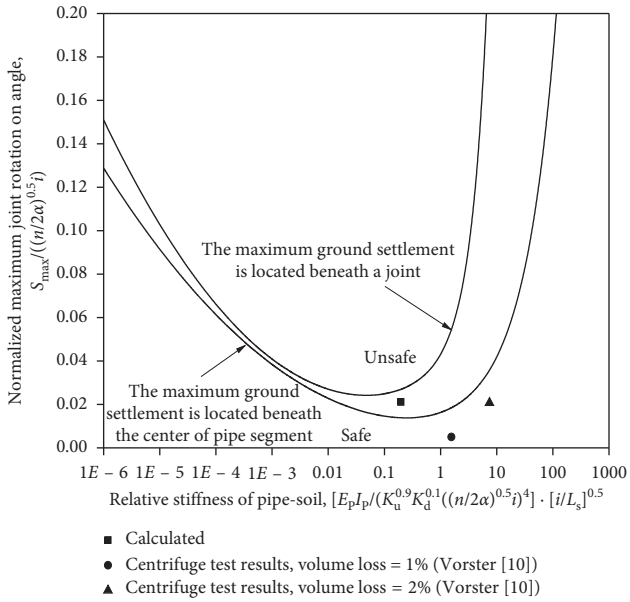

Figure 9: Illustration of the relationship between jointed pipeline safety criteria and the effects of tunnelling.

value moves closer to the dividing line. In other words, jointed pipelines gradually become unsafe as volume loss due to tunnelling increases. Figure 9 can be used directly to illustrate the relationship between the effects of tunnelling and jointed pipeline safety criteria.

9. Conclusions

(a) Jointed pipelines are most affected by the excavation of twin tunnels when the maximum ground settlement is beneath a joint and least affected when the maximum ground settlement is below the centre of a pipe segment.

(b) A dimensionless parameter, the relative pipe-soil stiffness, is proposed on the basis of calculations regarding the impact of twin-tunnel excavation on buried pipelines under different conditions.

(c) When the maximum ground settlement is located below a joint, the pipeline can be regarded as a flexible-jointed pipeline when the relative pipe-soil stiffness is less than 0.264 and as a stiff-jointed pipeline when the relative pipe-soil stiffness is above that value. When the maximum ground settlement is located below the centre of a pipe segment, this transition in pipeline behaviour occurs at a relative pipe-soil stiffness of 0.052.

(d) A regression equation describing the relationship between the relative pipe-soil stiffness and the normalized maximum joint rotation angle was estimated. This can be used to directly calculate the maximum joint rotation angle arising from single or twin tunnelling and, moreover, can be applied to evaluate tunnelling-induced risk to jointed pipelines.

Data Availability

The data used to support the findings of this study are included within the article.

Conflicts of Interest

The authors declare that they have no conflicts of interest.

Acknowledgments

The authors would like to acknowledge the financial supports of the National Natural Science Foundation of China (nos. 41362016, 51678166, and 51508113), the Guangxi Key Laboratory of Geomechanics and Geotechnical Engineering (no. 16-KF-01), and the Guangxi Key Laboratory of Disaster Prevention and Engineering Safety Systematic Research Project (2016ZDX003).

References

[1] A. K. Klar, A. M. M. M. Marshall, K. S. Soga, and R. J. M. J. Mair, "Tunnelling effects on jointed pipelines," *Canadian Geotechnical Journal*, vol. 45, no. 1, pp. 131–139, 2008.

[2] P. B. Attewell, J. Yeates, and A. R. Selby, *Soil Movements Induced by Tunnelling and Their Effects on Pipelines and Structures*, Methuen Inc, New York, NY, USA, 1986.

[3] J. Shi, Y. Wang, and C. W. W. Ng, "Numerical parametric study of tunneling-induced joint rotation angle in jointed pipelines," *Canadian Geotechnical Journal*, vol. 53, no. 12, pp. 2058–2071, 2016.

[4] B. P. Wham, M. C. Argyrou, and T. O'Rourke, "Jointed pipeline response to tunneling-induced ground deformation," *Canadian Geotechnical Journal*, vol. 53, no. 11, pp. 1794–1806, 2016.

[5] W. Gang, C. Wang, S. Cai et al., "Model test study on influence of quasi-rectangular shield construction on underground pipelines," *Chinese Journal of Geotechnical Engineering*, vol. 5, pp. 1–6, 2019.

[6] J. Shi, Y. Wang, and Y. Chen, "A simplified method to estimate curvatures of continuous pipelines induced by normal fault movement," *Canadian Geotechnical Journal*, vol. 53, no. 3, pp. 343–352, 2018.

[7] J. Shi, Y. Wang, and C. W. W. Ng, "Three-dimensional centrifuge modeling of ground and pipeline response to tunnel excavation," *Journal of Geotechnical and Geoenvironmental Engineering*, vol. 142, no. 11, article 04016054, 2016.

[8] Vorster and T. E. Beyerhaus, *The Effects of Tunnelling on Buried Pipes*, University of Cambridge, Cambridge, U.K, 2006.

[9] M. Saiyar, P. Ni, W. A. Take, and I. D. Moore, "Response of pipelines of differing flexural stiffness to normal faulting," *Géotechnique*, vol. 3, no. 4, pp. 1–12, 2015.

[10] T. E. B. Vorster, R. J. Mair, K. Soga, A. Klar, and P. J. Bennett, "Using BOTDR fiber optic sensors to monitor pipeline behavior during tunnelling," in *Proceedings of the European Workshop on Structural Health Monitoring*, pp. 930–937, Granada, Spain, July 2006.

[11] T. E. Vorster, A. Klar, K. Soga, and R. J. Mair, "Estimating the effects of tunneling on existing pipelines," *Journal of*

Geotechnical and Geoenvironmental Engineering, vol. 131, no. 11, pp. 1399–1410, 2005.

[12] A. M. Marshall, R. Farrell, A. Klar, and R. Mair, "Tunnels in sands: the effect of size, depth and volume loss on greenfield displacements," *Géotechnique*, vol. 62, no. 5, pp. 385–399, 2012.

[13] A. Klar and A. M. Marshall, "Linear elastic tunnel pipeline interaction: the existence and consequence of volume loss equality," *Géotechnique*, vol. 65, no. 9, pp. 788–792, 2015.

[14] S. Suwansawat and H. H. Einstein, "Describing settlement troughs over twin tunnels using a superposition technique," *Journal of Geotechnical and Geoenvironmental Engineering*, vol. 133, no. 4, pp. 445–468, 2007.

[15] A. M. Marshall, *Tunnelling in Sand and Its Effect on Pipelines and Piles*, University of Cambridge, Cambridge, U.K, 2009.

[16] C. H. Trautmann and T. D. O'Rourke, "Load-displacement characteristics of a buried pipe affected by permanent earthquake ground movements," *American Society of Mechanical Engineers, Pressure Vessels and Piping Division (Publication) PVP*, vol. 44, 1983.

[17] C. H. Trautmann, T. D. O'Rourfce, and F. H. Kulhawy, "Uplift force-displacement response of buried pipe," *Journal of Geotechnical Engineering*, vol. 111, no. 9, pp. 1061–1076, 1985.

[18] American Society of Civil Engineers and Committee on Gas and Liquid Fuel Lifelines, *Guidelines for the Seismic Design of Oil and Gas Pipeline Systems*, American Society of Civil Engineers, Reston, VA, USA, 1984.

[19] D. G. Honegger, R. W. Gailing, and D. J. Nyman, "Guidelines for the seismic design and assessment of natural gas and liquid hydrocarbon pipelines," in *Proceedings of the 4th International Pipeline Conference*, pp. 563–570, American Society of Mechanical Engineers, Calgary, Canada, September-October 2002.

[20] M. Balkaya, I. D. Mooreb, and A. Sağlamer, "Study of non-uniform bedding due to voids under jointed PVC water distribution pipes," *Geotextiles & Geomembranes*, vol. 34, no. 10, pp. 39–50, 2012.

[21] J. Kim, S. S. Nadukuru, M. Pour-Ghaz et al., "Assessment of the behavior of buried concrete pipelines subjected to ground rupture: experimental study," *Journal of Pipeline Systems Engineering and Practice*, vol. 3, no. 1, pp. 8–16, 2012.

[22] K. M. Molnar, R. J. Finno, and E. C. Rossow, "Analysis of effects of deep braced excavations on adjacent buried utilities," Report for the U.S. Department of Transportation, No. A450, A464, Northwestern University, Evanston, IL, USA, 2003.